MUON $g-2$ AND LEPTON-FLAVOUR VIOLATION IN THE MRSSM*

Wojciech Kotlarski, Dominik Stöckinger
Hyejung Stöckinger-Kim

Institut für Kern- und Teilchenphysik, TU Dresden
01069 Dresden, Germany

(Received November 8, 2019)

We present a recent study of the muon magnetic moment and two lepton-flavour violating observables in the MRSSM. The MRSSM exhibits several key differences compared to the MSSM: there is no $\tan\beta$ enhancement in $(g-2)$ or $\mu \to e\gamma$, and the correlation between $\mu \to e\gamma$ and $\mu \to e$ conversion is weak in the largest region of parameter space. As a result, the MRSSM can be falsified if the COMET Phase 1 experiment finds a non-vanishing signal.

DOI:10.5506/APhysPolB.50.1921

1. Introduction

Low-energy lepton observables provide appealing ways to test the Standard Model and to identify and constrain potential new physics. Here, we consider three such observables. One of them is the muon magnetic moment $a_\mu = (g-2)_\mu/2$. Using the recent SM theory evaluation of the KNT Collaboration [1], the deviation from the Brookhaven measurement [2] is given by

$$\Delta a_\mu^{\mathrm{Exp-SM}} = (27.06 \pm 7.26) \times 10^{-10}\,. \tag{1}$$

This constitutes a tantalizing 3–4σ discrepancy which might be due to new physics. The ongoing $(g-2)$ measurement at Fermilab will significantly improve the experimental precision by up to a factor four [3]. It thus has the potential to sharpen the need for new physics.

In addition we consider two lepton-flavour violating observables, the decay $\mu \to e\gamma$ and the $\mu \to e$ conversion in a muonic atom. The current experimental upper limits on the corresponding branching/conversion ratios from the MEG and SINDRUM experiments are [4, 5]

* Presented at the XLIII International Conference of Theoretical Physics "Matter to the Deepest", Chorzów, Poland, September 1–6, 2019.

$$B_{\mu^+ \to e^+ \gamma} \; < \; 4.2 \times 10^{-13} \; (90\%\text{C.L.})\,. \tag{2}$$

$$B_{\mu\mathrm{Au} \to e\mathrm{Au}} \; < \; 7 \times 10^{-13} \; (90\%\text{C.L.})\,. \tag{3}$$

Particularly important progress will soon be made by the COMET [6, 7] experiment, which will measure $\mu \to e$ conversion in an aluminium nucleus with foreseen limits of 7.2×10^{-15} for COMET Phase 1 and better than 10^{-16} for COMET Phase 2.

Among all ideas for physics beyond the Standard Model, supersymmetry is especially well-motivated. However, supersymmetry does not have to be realized in the form of the "Minimal Supersymmetric Standard Model" (MSSM). In fact, supersymmetry can be made even more attractive by combining it with R-symmetry, the U(1)-symmetry allowed by the supersymmetry algebra under which particles and SUSY partners have *different* charges. The minimal R-symmetric supersymmetric model is called MRSSM [8]. It provides a realization of supersymmetry which is distinct from the MSSM — neither does the MRSSM have an MSSM limit nor has the MSSM and MRSSM limit. A key difference is that gauginos and Higgsinos are R-charged and have Dirac instead of Majorana masses. Therefore, the MRSSM has more degrees of freedom than the MSSM, but fewer free parameters, thanks to the additional symmetry!

In previous studies, the phenomenology of the MRSSM was found to be surprisingly rich and successful [9–13]. Here, we report on Ref. [14] where we ask: What are the possible MRSSM contributions to $(g-2)_\mu$ and to the two lepton-flavour violating observables? And what are the correlations between these contributions? We note that in the usual MSSM, contributions to $(g-2)_\mu$ are $\tan\beta$-enhanced and all three observables are strongly correlated, see *e.g.* [15, 16]. First investigations of lepton-flavour violation in the MRSSM in [17] have indicated a different pattern.

2. Key properties

To be precise, the MRSSM contains the same superfields as the MSSM, plus additional superfields containing the Dirac mass partners of the gauginos and Higgsinos. These are the superfields $\hat{O}$ (octino, octet), $\hat{T}$ (triplino, triplet), $\hat{S}$ (singlino, singlet), with R-charge 0 and $\hat{R}_{d,u}$ (R-Higgsinos, R-Higgs fields) with R-charge $+\,2$. A relevant excerpt of the MRSSM superpotential is given by

$$W = \Lambda_d\, \hat{R}_d \cdot \hat{T}\, \hat{H}_d \, + \lambda_d\, \hat{S}\, \hat{R}_d \cdot \hat{H}_d \, - Y_e\, \hat{e}\, \hat{l} \cdot \hat{H}_d\,. \tag{4}$$

The last of these terms is the MSSM-like lepton Yukawa coupling; the other terms are MRSSM-specific, new Yukawa-like terms connecting (R)-Higgsinos with triplet or singlet superfields. Similar terms exist with up-type fields. Importantly, the MSSM μ-term $\mu\hat{H}_u\hat{H}_d$ is forbidden in the MRSSM.

The MRSSM-specific parameters $\lambda_{u,d}$ and $\Lambda_{u,d}$ have already played an important role in the study of electroweak phenomena in Ref. [9], where they act similarly to the top-Yukawa coupling to increase the mass of the Higgs boson and to give dominant contributions to electroweak precision observables.

For our study of lepton observables, a key difference between the MRSSM and the MSSM is the absence of $\tan\beta$-enhancements to the magnetic dipole operators. Figure 1 shows mass-insertion diagrams for a_μ in the MSSM and MRSSM. The $\tan\beta$-enhancement present in the MSSM originates from Feynman diagrams where an effective coupling of leptons to the up-type Higgs VEV v_u is generated. This can happen in the MSSM in one-loop diagrams involving the μ-parameter and the Majorana gaugino masses. However, in the MRSSM, μ and Majorana masses are zero because of R-symmetry. As a result, there are no one-loop diagrams generating an effective coupling to v_u. The middle diagram of Fig. 1 shows a typical MRSSM diagram which is not enhanced by anything.

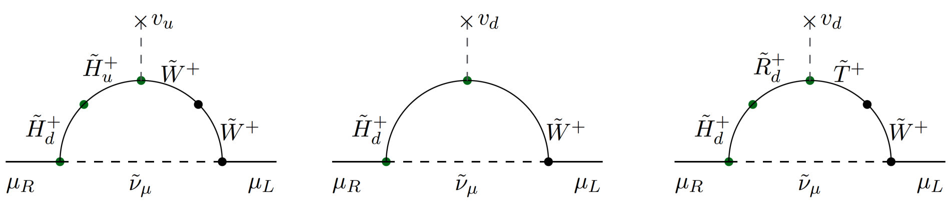

Fig. 1. Sketch of mass insertion diagrams for $(g-2)_\mu$ in the MSSM (left) and the MRSSM (middle and right).

However, the right diagram of Fig. 1 shows a possible enhancement mechanism in the MRSSM: Instead of a coupling to v_u, this diagram shows an enhanced coupling to v_d, where the enhancement originates from the new Yukawa-like Λ_d parameter. The different behaviour of the two leading kinds of mass-insertion diagrams in the MSSM and the MRSSM can be summarized as

$$\begin{aligned} a_\mu^{\text{MSSM,WHL}} &\approx \frac{g_2^2\tan\beta}{16\pi^2}\frac{5}{12}\frac{m_\mu^2}{M_{\text{SUSY}}^2}\,, \\ a_\mu^{\text{MRSSM,WHL/cn}} &\approx \frac{g_2\Lambda_d}{16\pi^2}\frac{5}{12}\frac{m_\mu^2}{M_{\text{SUSY}}^2}\,, \end{aligned} \tag{5}$$

where the labels correspond to the particles appearing in the diagrams, g_2 is the $\mathrm{SU}(2)_L$ gauge coupling and M_{SUSY} denotes the generic SUSY mass scale. Similar results are obtained for mass insertion diagrams involving the bino/singlino and right-handed sleptons; such diagrams can be enhanced by the parameter λ_d.

Thus, the key difference between the MRSSM and MSSM is that the $\tan\beta$-enhancement of the MSSM is replaced by a Λ_d, λ_d-enhancement in the MRSSM. We recall that the Λ_d, λ_d-parameters are Yukawa-like parameters. Thus, values around unity are possible, but values above $\sqrt{4\pi}$ are disfavoured by perturbativity. Hence, the possible dipole enhancement in the MRSSM is much weaker than in the MSSM.

3. Results for a_μ in the MRSSM

Let us now discuss the possible values of the MRSSM contributions to a_μ. As shown above, the contributions have an overall suppression by $1/M^2_{\rm SUSY}$ where $M_{\rm SUSY}$ is the scale of the relevant SUSY masses; there can be an enhancement by the Yukawa-like parameters Λ_d, λ_d, but in order to invoke such an enhancement, all SUSY masses appearing in the corresponding mass-insertion diagrams need to be small: this means that large contributions require at least three light SUSY masses, among them at least one smuon, one gaugino, and one Higgsino.

Figure 2 shows the possible values for a_μ in the MRSSM, resulting from a scan over the MRSSM parameter space. The possible values are plotted as a function of the lightest observable (*i.e.* lightest electrically charged) SUSY particle mass, and the Λ_d, λ_d parameters are restricted in various ways as indicated in the plot. The plot shows indeed that a_μ in the MRSSM is significantly smaller than in the MSSM. The currently observed discrepancy in a_μ can only be accommodated in a specific parameter region of the MRSSM: at least one of the Λ_d, λ_d must be close to the perturbativity limit and much larger than the gauge couplings, and several SUSY masses need to be around or below 200 GeV.

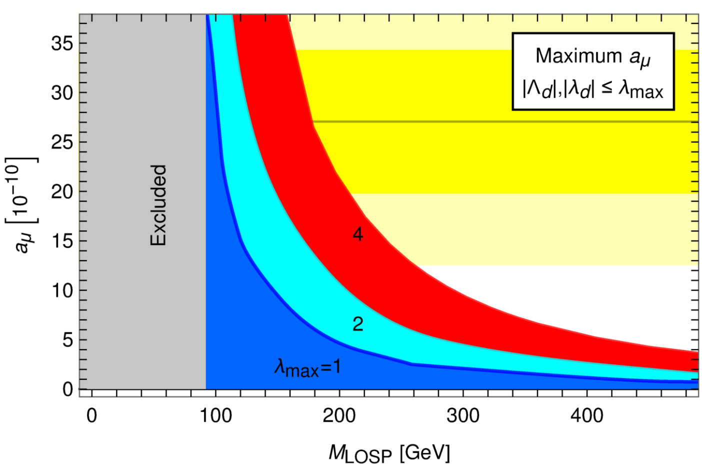

Fig. 2. Possible values of a_μ in the MRSSM, from [14].

4. Results for lepton-flavour violating observables in the MRSSM

Now, we consider also two lepton-flavour violating observables: the decay $\mu \to e\gamma$ and muon-to-electron conversion $\mu \to e$ in the presence of a nucleus. Some key points to notice are:

— Like a_μ, the decay $\mu \to e\gamma$ is governed by dipole amplitudes $A_2^{\bar{l}\mu\mathrm{L/R}}$, where $l = e, \mu$ and where L/R denotes the chirality of l. Thus the two observables depend on the same parameters, except the *additional* dependence of $\mu \to e\gamma$ on the flavour-violating parameters

$$\delta_{12}^{\mathrm{L}} \equiv \frac{\left(m_{\tilde{l}}^2\right)_{12}}{m_{\tilde{l},11} m_{\tilde{l},22}}\,, \qquad \delta_{12}^{\mathrm{R}} \equiv \frac{\left(m_{\tilde{e}}^2\right)_{12}}{m_{\tilde{e},11} m_{\tilde{e},22}}\,.$$

The flavour-violating amplitudes are essentially linear in these parameters; hence, we can write the following approximate relations

$$B_{\mu\to e\gamma} \propto \left|A_{2\mathrm{red}}^{\bar{e}\mu\mathrm{L}}\right|^2 \times \left|\delta_{12}^{\mathrm{L}}\right|^2 + \left|A_{2\mathrm{red}}^{\bar{e}\mu\mathrm{R}}\right|^2 \times \left|\delta_{12}^{\mathrm{R}}\right|^2 , \tag{6}$$

$$a_\mu \propto A_2^{\bar{\mu}\mu\mathrm{L}} + A_2^{\bar{\mu}\mu\mathrm{R}} . \tag{7}$$

This highlights that we can expect very strong correlations particularly if either the left-handed or the right-handed amplitudes dominate. The correlation is weakened in the case of destructive interferences within a_μ or in the case of strong hierarchies between the parameters $\delta_{12}^{\mathrm{L/R}}$.

— Muon-to-electron conversion, on the other hand, has a more complicated structure. It is given not only in terms of dipole amplitudes but also in terms of photon charge radius, Z penguin, and box amplitudes. In the MSSM, the dipole amplitude usually dominates and $\mu \to e$ is strongly correlated with $\mu \to e\gamma$ and a_μ. In the MRSSM, however, this is only the case in the small region of parameter space with enhanced dipole. The more natural expectation in the MRSSM is that there is only a weak correlation between $\mu \to e$ conversion and $\mu \to e\gamma$.

One way to make use of the correlation between $\mu \to e\gamma$ and a_μ is shown in Fig. 3, where we ask the following question: Suppose, the MRSSM explains the discrepancy in a_μ within the 1σ-level, then which values of the δs are allowed by the MEG-limit (2)? Figure 3 shows the answer encoded in traffic-light colours. The small grey/green ellipse indicates values of the δs which are always allowed, no matter how a_μ is explained in the MRSSM. These always allowed values are of the order of 10^{-5} or smaller. On the other hand, the pale grey/yellow area indicates values of the δs which are sometimes allowed and sometimes forbidden, depending on how a_μ is explained (*e.g.* predominantly by left-handed or by right-handed amplitudes or predominantly by terms enhanced by λ_d or by Λ_d). This area is the area probed by the MEG-limit. The dark grey/red area is already fully excluded by the MEG-limit (under the given assumption on a_μ). The excluded parameter space reaches values of the δ's down to 10^{-4}.

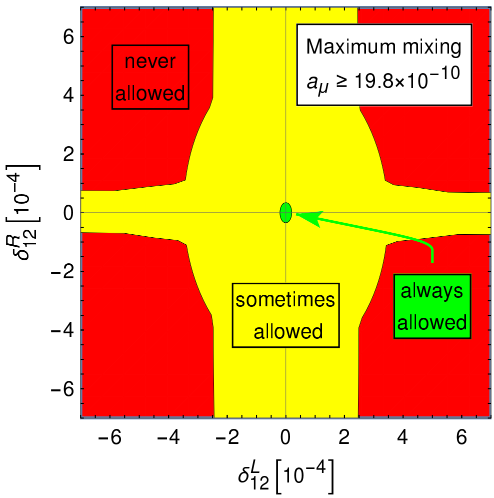

Fig. 3. Traffic-light-plot showing the maximum values of the δ-parameters compatible with the MEG-limit, under the assumption that the MRSSM explains the currently observed a_μ discrepancy. From [14].

The best way to investigate the behaviour of muon-to-electron conversion in the MRSSM is to study the ratio

$$R(N) \equiv \frac{B_{\mu N\to eN}}{B_{\mu\to e\gamma}} \tag{8}$$

which depends on the chosen nucleus. In the case of dipole dominance, this ratio simply becomes a model-independent constant: in the case of aluminium Ref. [18] obtained

$$R^{\text{only dip}}(\text{Al}) = 0.0026\,. \tag{9}$$

Any deviation from this is a signal and measure of the impact of the non-dipole contributions to $\mu\to e$ conversion.

Figure 4 shows the possible values of $R(\text{Al})$ in the MRSSM. The values are shown as a function of the value of a_μ. The prediction for dipole dominance (allowing a factor 2 up or down) is indicated by the lightest grey/light blue shading at the bottom of the figure. We find the expected behaviour: if the MRSSM contributions to a_μ are large, we are forced to the small parameter region with enhanced dipole contributions, and in this parameter region, the dipoles are the dominant contributions to $\mu \to e$ conversion — hence, the ratio R is close to the prediction for dipole dominance, and $\mu \to e$ conversion is strongly correlated with $\mu \to e\gamma$.

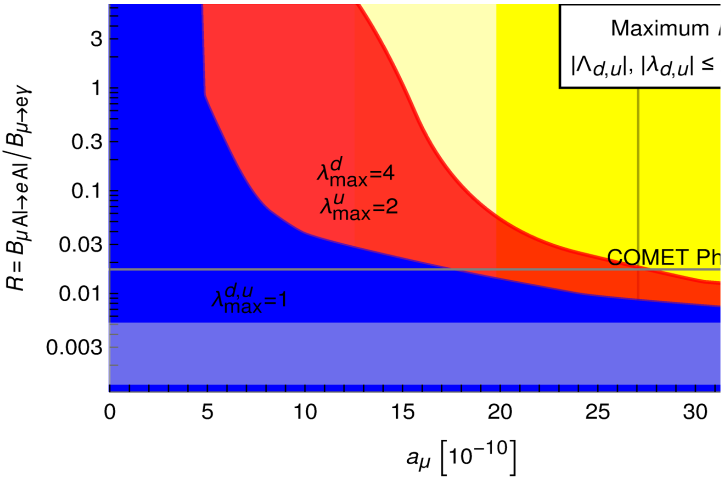

Fig. 4. Correlation between $\mu \to e$ conversion and $\mu \to e\gamma$, from [14].

If, on the other hand, a_μ is small in the MRSSM, then the correlation between $\mu \to e$ conversion and $\mu \to e\gamma$ is weak.

The figure also shows a horizontal line indicating the reach of COMET Phase 1, taking into account the current MEG-limit. We see that COMET Phase 1 has a strong sensitivity to MRSSM contributions, provided that a_μ is small.

5. Conclusions

In conclusion, the MRSSM is a distinctive SUSY model which challenges several usual views on SUSY. It is a phenomenologically rich and successful model which does not possess an MSSM limit and which is viable for rather light SUSY masses. Here, we have discussed the study [14] of the three observables a_μ, $\mu \to e\gamma$, $\mu \to e$ conversion and their interplay.

Most importantly, dipole amplitudes have no $\tan\beta$ enhancement in the MRSSM — hence, contributions to a_μ are significantly smaller than in the MSSM. However, there is a milder enhancement in the case of large parameters Λ_d, λ_d, which allows to accommodate the current a_μ discrepancy if several SUSY masses are below 200 GeV. The correlation between a_μ and $\mu \to e\gamma$ is similar as in the MSSM. Here, it has allowed to produce Fig. 3, showing maximum allowed flavour-mixing parameters in the MRSSM.

The correlation with $\mu \to e$ conversion is strong only if a_μ is large. In this case, current MEG-limits on $\mu \to e\gamma$ already imply that the forthcoming COMET Phase 1 measurement will not be sensitive to the MRSSM.

However, in the case when the MRSSM contributions to a_μ are smaller, the situation is very different. In this case, the correlation between the two lepton-flavour violating observables is very weak, and COMET Phase 1 has a strong sensitivity to the MRSSM.

Conversely, if COMET discovers a signal for $\mu \to e$ conversion, and forthcoming a_μ measurements confirm the current discrepancy, the MRSSM will be excluded!

REFERENCES

[1] A. Keshavarzi, D. Nomura, T. Teubner, *Phys. Rev. D* **97**, 114025 (2018) [arXiv:1802.02995 [hep-ph]].

[2] G.W. Bennett *et al.* [Muon $g-2$ Collab.], *Phys. Rev. D* **73**, 072003 (2006) [arXiv:hep-ex/0602035].

[3] J. Grange *et al.* [Muon $g-2$ Collab.], arXiv:1501.06858 [physics.ins-det].

[4] A.M. Baldini *et al.* [MEG Collab.], *Eur. Phys. J. C* **76**, 434 (2016) [arXiv:1605.05081 [hep-ex]].

[5] W.H. Bertl *et al.* [SINDRUM II Collab.], *Eur. Phys. J. C* **47**, 337 (2006).

[6] Y.G. Cui *et al.* [COMET Collab.], KEK-2009-10.

[7] Y. Kuno [COMET Collab.], *Prog. Theor. Exp. Phys.* **2013**, 022C01 (2013).

[8] G.D. Kribs, E. Poppitz, N. Weiner, *Phys. Rev. D* **78**, 055010 (2008) [arXiv:0712.2039 [hep-ph]].

[9] P. Dießner, J. Kalinowski, W. Kotlarski, D. Stöckinger, *J. High Energy Phys.* **1412**, 124 (2014) [arXiv:1410.4791 [hep-ph]].

[10] P. Diessner, J. Kalinowski, W. Kotlarski, D. Stöckinger, *Adv. High Energy Phys.* **2015**, 760729 (2015) [arXiv:1504.05386 [hep-ph]].

[11] P. Diessner, J. Kalinowski, W. Kotlarski, D. Stöckinger, *J. High Energy Phys.* **1603**, 007 (2016) [arXiv:1511.09334 [hep-ph]].

[12] P. Diessner, W. Kotlarski, S. Liebschner, D. Stöckinger, *J. High Energy Phys.* **1710**, 142 (2017) [arXiv:1707.04557 [hep-ph]].

[13] P. Diessner, J. Kalinowski, W. Kotlarski, D. Stöckinger, *J. High Energy Phys.* **1909**, 120 (2019) [arXiv:1907.11641 [hep-ph]].

[14] W. Kotlarski, D. Stöckinger, H. Stöckinger-Kim, *J. High Energy Phys.* **1908**, 082 (2019) [arXiv:1902.06650 [hep-ph]].

[15] D. Stöckinger, *J. Phys. G* **34**, R45 (2007).

[16] L. Calibbi *et al.*, *J. High Energy Phys.* **1510**, 043 (2015) [arXiv:1502.07753 [hep-ph]].

[17] R. Fok, G.D. Kribs, *Phys. Rev. D* **82**, 035010 (2010) [arXiv:1004.0556 [hep-ph]].

[18] R. Kitano, M. Koike, Y. Okada, *Phys. Rev. D* **66**, 096002 (2002) [*Erratum ibid.* **76**, 059902 (2007)] [arXiv:hep-ph/0203110].